

# 1:2 Formic Acid/Acetylene Complexes: Ab Initio and Matrix Isolation Studies of Weakly Interacting Systems

Elsa Sánchez-García,<sup>†</sup> Lisa George,<sup>†</sup> Luis A. Montero,<sup>‡</sup> and Wolfram Sander<sup>\*,†</sup>

*Lehrstuhl für Organische Chemie II, Ruhr-Universität Bochum, D-44780 Bochum, Germany, and Laboratorio de Química Computacional y Teórica, Facultad de Química, Universidad de la Habana, 10400 Havana, Cuba*

*Received: April 5, 2004; In Final Form: September 7, 2004*

The complexes formed by noncovalent interactions between one molecule of formic acid and two molecules of acetylene are investigated by DFT and ab initio methods and characterized by matrix isolation spectroscopy. Six complexes with binding energies between  $-3.93$  and  $-7.98$  kcal/mol (MP2/cc-pVTZ + ZPE) are identified. The three most strongly bound complexes are found within a range of 1 kcal/mol. The binding interactions in these complexes are  $\text{OH}\cdots\pi$ ,  $\text{CH}\cdots\pi$ , and  $\text{CH}\cdots\text{O}$  interactions that can be classified as weak hydrogen bonds. The competition between these weak hydrogen bonds is discussed in detail. Matrix isolation spectroscopy allowed for the characterization of the most strongly bound complex by its IR spectrum.

## Introduction

During the past several years, the weak hydrogen bonding involving a hydrogen atom bound to a carbon atom as hydrogen donor has attracted attention from the scientific community. It was found that these weak interactions play important roles in molecular recognition, properties of condensed phases, solid-state reactions, and crystal engineering and in determining the shapes and stabilities of biomolecules.<sup>1–5</sup> In contrast to the conventional strong hydrogen bonds, which have been extensively described, the nature and characteristics of weak noncovalent interactions do not comprise a well-resolved field. Thus, experimental and theoretical studies of  $\text{CH}\cdots\text{O}$  and  $\text{C}-\text{H}\cdots\pi$  interactions are of key interest for the understanding of biological and chemical systems.

A number of studies have been published on the weak interactions in complexes or dimers of hydrocarbons with  $\pi$  systems such as acetylene, benzene, and ethylene.<sup>6–12</sup> The dimer of acetylene has been investigated both experimentally and theoretically,<sup>13–20</sup> and a  $\pi$ -type hydrogen-bonded  $\text{C}_{2v}$  minimum was found, together with several first- and second-order saddle points.<sup>21–25</sup> The proton-transfer mechanism of strong hydrogen-bonded systems such as the formic acid dimer has also been extensively studied.<sup>26–33</sup> Studies of 1:1 formic acid/acetylene complexes were carried out using matrix isolation and theoretical methods.<sup>34</sup>

In this work, the trimers formed by the interaction of one molecule of formic acid with two molecules of acetylene (1:2 formic acid/acetylene complexes) are investigated using both theoretical methods and matrix isolation techniques. The characterization of trimer complexes is a challenge both for theory and for experiment. These complexes consisting of three molecules allow for a detailed analysis of the influence of a third molecule on the properties of the dimer, e.g., of an additional acetylene molecule on the acetylene/formic acid dimer or of a formic acid molecule on the acetylene dimer. An interesting feature of this system is the competition between

the strongly acidic carboxyl group, the acetylene group, and the formyl group as hydrogen bridge donors and the carbonyl group, the hydroxyl group, and the acetylene  $\pi$  system as hydrogen bridge acceptors. This leads to a large number of complexes with strong  $\text{OH}\cdots\text{O}$  and weak  $\text{CH}\cdots\text{O}$  or  $\text{CH}\cdots\pi$  hydrogen bridges. Because of the large number of complexes with similar binding energies, a careful search for minima on the potential energy surface is mandatory.

## Experimental Section

Matrix isolation experiments were performed by standard techniques using an APD CSW-202 Displex closed-cycle helium refrigerator. Spectroscopic-grade formic acid (Acros Organics) and acetylene/deuterated acetylene were premixed with argon in a gas mixing chamber made of glass using standard manometric methods. Formic acid was degassed several times by the freeze–pump–thaw method before being mixed with argon. About 1–4 mbar of acetylene/deuterated acetylene was mixed with 0.5–2 mbar of formic acid and diluted with 800 mbar of argon in a 2-L glass bulb. Deposition was done on a CsI substrate held at 15 K. The matrix was annealed at 30 K by maintaining that temperature for 20 min and then cooling to 15 K before recording the annealed spectra. Spectra were recorded with Bruker Equinox 55 and IFS/66V FTIR spectrometers at  $0.5\text{ cm}^{-1}$  resolution in the range of  $400\text{--}4000\text{ cm}^{-1}$ , and 128 scans were co-added.

## Computational Methods

The multiple minima hypersurface (MMH) approach<sup>34–36</sup> was used to localize the minima for the 1:2 formic acid/acetylene system. One thousand randomly arranged 1:2 formic acid/acetylene clusters were generated as starting points in each case, and a traditional gradient minimization procedure was used with semiempirical Hamiltonians to reach minima in such hypersurfaces. All resulting energies and geometries were processed with two programs specifically written for this purpose. The most relevant minima arrangements of 1:2 formic acid/acetylene complexes were taken for further optimizations at higher levels of theory. PM3 and AM1<sup>37–39</sup> approximate quantum mechanical Hamiltonians were used. Because the limitations of semiem-

\* To whom correspondence should be addressed. E-mail: wolfram.sander@rub.de.

<sup>†</sup> Ruhr-Universität Bochum.

<sup>‡</sup> Universidad de la Habana.

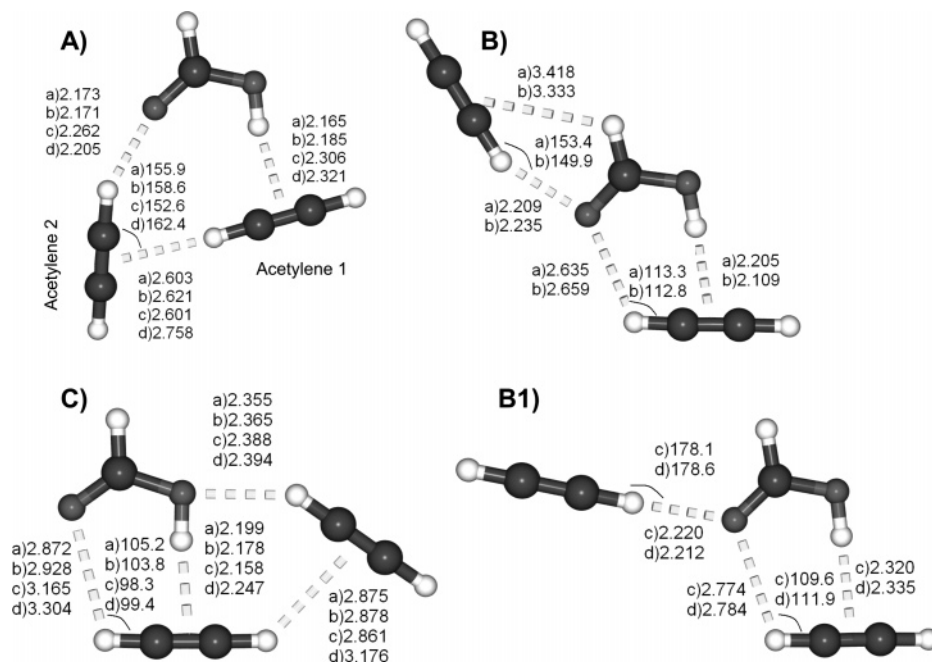


**Figure 1.** Calculated structures with hydrogen-bond lengths and some hydrogen-bond angles of 1:2 formic acid/acetylene complexes **A**, **B**, **C**, and **B1**. (a) MP2/cc-pVTZ, (b) MP2/6-311++G(3df,3pd), (c) MP2/6-311++G(d,p), (d) B3LYP/6-311++G(d,p).

pirical Hamiltonians are well-known,<sup>2,4,40–42</sup> it is convenient to remark that, in our case, such calculations are performed only for providing a very early criterion for geometric discrimination before further DFT and ab initio optimizations. Both PM3 and AM1 methods lead to the same minima after geometrical discrimination analysis and additional optimizations of the geometries.

Ab initio and DFT computations were performed using the Gaussian 98,<sup>43</sup> Gaussian 03,<sup>44</sup> and MOLPRO<sup>45</sup> programs. The equilibrium geometries and vibrational frequencies were calculated at the SCF level with second-order Møller–Plesset perturbation theory, MP2,<sup>46</sup> and the DFT level with the B3LYP hybrid functional.<sup>47,48</sup> For complexes **A–C**, single-point calculations were performed with coupled clusters<sup>49</sup> of single and double substitutions (with noniterative triples), CCSD(T)/cc-pVTZ.

For the MP2 calculations, both Pople's triple- $\zeta$  basis set augmented with diffuse and polarization functions, 6-311++G(d,p), and Dunning's correlation consistent triple- $\zeta$  basis set, cc-pVTZ,<sup>50–52</sup> were used to avoid problems with basis set superposition error (BSSE). In addition, at the MP2/cc-pVTZ level of theory, the binding energies for complexes **A–C** were corrected for BSSE using the counterpoise (CP) scheme of Boys and Bernardi.<sup>53</sup> With these basis sets and in accordance with our previous experience with the 1:1 formic acid/acetylene complexes,<sup>34</sup> significant effects of BSSE on the energies and geometries of the complexes were not expected.

To evaluate the effect of the size of the basis set in MP2 calculations, the strongly polarized basis set 6-311++G(3df,3pd) (381 basis functions) was used, and the results obtained were compared to those of MP2 calculations with the cc-pVTZ (294 basis functions) and 6-311++G(d,p) (196 basis functions) basis sets. B3LYP/6-311++G(d,p) calculations were used only for initial geometry optimizations. The DFT results are presented for comparison with the MP2 and CCSD(T) data. The stabilization energies were calculated by subtracting the energies of the monomers from those of the complexes and including ZPE corrections to discard other than electronic terms in the energy comparisons.

## Results and Discussion

**Geometries and Binding Energies.** The binding in complexes between formic acid and acetylene shows contributions from the following five basic binding motifs: (i) OH $\cdots\pi$  interaction between the acidic H atom of formic acid and the  $\pi$  system of acetylene, (ii) CH $\cdots\pi$  interaction between the formyl H atom of formic acid and the  $\pi$  system of acetylene, (iii) CH $\cdots\pi$  interaction between one acetylene H atom and the  $\pi$  system of the second acetylene molecule, (iv) CH $\cdots$ O interaction between one acetylene H atom and the carbonyl oxygen atom of formic acid, and (v) CH $\cdots$ O interaction between one acetylene H atom and the hydroxyl oxygen atom of formic acid.

In the following discussion, we describe and quantify the structures and binding energies of the complexes between one molecule of formic acid and two molecules of acetylene with respect to these binding contributions. To avoid confusion between the two molecules of acetylene in complexes, we call the acetylene with the  $\pi$  system directly interacting with the O–H group acetylene 1 and the second acetylene molecule acetylene 2. In complexes **D–G**, the acetylene molecule with the  $\pi$  system interacting with the C–H group of the formic acid is called acetylene 1.

Six complexes (**A–G**) corresponding to local minima between one molecule of formic acid and two molecules of acetylene were found at the MP2/cc-pVTZ level of theory. Four additional structures, **B1**, **E1**, **G1**, and **H1**, were located using DFT theory [B3LYP/6-311++G(d,p)] or MP2 with a smaller basis set [MP2/6-311++G(d,p)], but are not minima at higher levels of theory (Figures 1 and 2). At all levels of theory, complex **A** is predicted to be the global minimum, followed by complexes **B** and **C** (Tables 1–3). At the CCSD(T)/cc-pVTZ//MP2/cc-pVTZ level of theory, after ZPE corrections, the calculated binding energy for complex **A** is  $-7.44$  kcal/mol, and the binding energies for complexes **B** and **C** are  $-6.85$  and  $-6.47$  kcal/mol, respectively. Thus, three stable complexes with binding energies within 1 kcal/mol are predicted.

At the MP2 level of theory, the calculated binding energies and geometries are not very dependent on the size of the basis set. For complex **A**, using the 6-311G++(d,p), cc-pVTZ, and

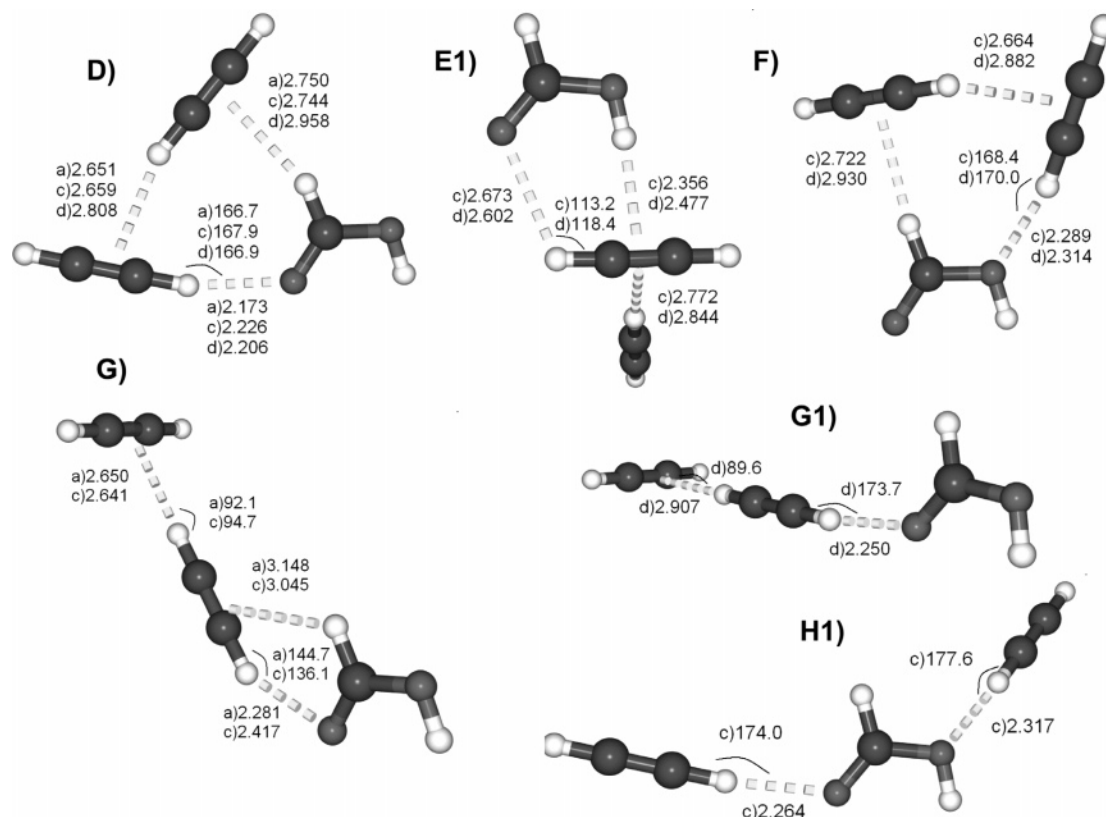


**Figure 2.** Calculated structures with hydrogen-bond lengths and some hydrogen-bond angles of 1:2 formic acid/acetylene complexes: **D**, **F**, **G**, **E1**, **G1**, and **H1**. (a) MP2/cc-pVTZ, (c) MP2/6-311++G(d,p), (d) B3LYP/6-311++G(d,p).

**TABLE 1: Calculated Binding Energies and ZPE-Corrected Values of the 1:2 Formic Acid/Acetylene Complexes A–D, F, and G (in kcal/mol)**

complex	B3LYP/ 6-311++G(d,p)		MP2/ 6-311G++(d,p)		MP2/cc-pVTZ		
	$\Delta E$	$\Delta E_{\text{(ZPE)}}$	$\Delta E$	$\Delta E_{\text{(ZPE)}}$	$\Delta E$	$\Delta E_{\text{(ZPE)}}$	$\Delta E_{\text{(BSSE)}}$
<b>A</b>	−6.58	−4.95	−9.23	−7.64	−9.52	−7.98	−7.87
<b>B</b>					−8.77	−7.18	−6.84
<b>C</b>	−5.12	−3.80	−8.03	−6.63	−8.42	−7.05	−6.73
<b>D</b>	−4.43	−2.98	−7.00	−5.27	−6.79	−5.47	
<b>F</b>	−3.06	−1.85	−6.02	−4.33	−5.37	−4.32	
<b>G</b>			−5.01	−3.65	−5.06	−3.93	

**TABLE 2: MP2 and CCSD(T) Calculated Binding Energies for the Complexes A–C<sup>a</sup>**

complex	MP2/ 6-311G++(3df,3pd)		CCSD(T)/ cc-pVTZ//MP2/cc-pVTZ	
	$\Delta E$	$\Delta E_{\text{(ZPE)}}$	$\Delta E$	$\Delta E_{\text{(ZPE)}}$
<b>A</b>	−9.83	−8.29	−8.98	−7.44
<b>B</b>	−8.62	−7.03	−8.44	−6.85
<b>C</b>	−8.53	−7.16	−7.84	−6.47

<sup>a</sup> ZPE corrections are from the MP2/cc-pVTZ calculations.

6-311G++(3df,3pd) basis sets, the binding energies after ZPE corrections are −7.64, −7.98, and −8.29 kcal/mol, respectively. B3LYP computations predict greater binding energies than MP2. At all levels of theory and in accordance with qualitative expectations, complexes **D–G** are less stable than complexes **A–C** (Table 1 and Figures 1 and 2). The MP2 geometries and binding energies calculated with the cc-pVTZ and the 6-311++G-(3df,3pd) basis sets are quite similar. However, the geometries obtained with the smaller 6-311++G(d,p) basis set differ significantly from the cc-pVTZ results. The MP2/cc-pVTZ level of theory has been established as quite adequate for calculating properties of weakly interacting systems, as has been confirmed

**TABLE 3: Calculated Binding Energies and ZPE-Corrected Values of 1:2 Formic Acid/Acetylene Complexes B1, E1, G1, and H1 (in kcal/mol)**

complex	B3LYP/ 6-311++G(d,p)		MP2/ 6-311G++(d,p)		MP2/ cc-pVTZ	
	$\Delta E$	$\Delta E_{\text{(ZPE)}}$	$\Delta E$	$\Delta E_{\text{(ZPE)}}$	$\Delta E$	$\Delta E_{\text{(ZPE)}}$
<b>B1</b>	−6.08	−4.55	−7.91	−6.06		B <sup>a</sup>
<b>E1</b>	−4.15	−2.92	−6.63	−4.94		C <sup>a</sup>
<b>G1</b>	−3.12	−1.98				G <sup>a</sup>
<b>H1</b>	−4.48	−3.24	−5.03	−3.00		D <sup>a</sup>

<sup>a</sup> See Table 1.

by calculations of molecular systems with similar types interactions, such as the 1:1 formic acid/acetylene complexes<sup>34</sup> and the acetylene dimers studies by Karpfen.<sup>21</sup> The good performance of the cc-pVTZ basis set for these systems also suggests that this more economical basis set can be used instead of the 6-311++G(3df,3pd) basis set. For complexes **A–C**, the BSSE-corrected binding energies at the MP2/cc-pVTZ level of theory are also listed (Table 1). As expected, the BSSE contributions are of minimal significance for the calculated binding energies.

In complex **A**, the acidic hydrogen atom of the formic acid molecule interacts with the  $\pi$  system of one molecule of acetylene (contribution i). The MP2-calculated distance of the C1 carbon atom of acetylene from the acidic hydrogen atom of formic acid (OH...C1 distance) is 2.293 Å (2.301 Å), and that of C2 (OH...C2 distance) is 2.297 Å (2.307 Å) using a cc-pVTZ [6-311++G(3df,3pd)] basis set. The carbonyl oxygen atom of formic acid interacts with one hydrogen atom of the second acetylene molecule (contribution iv) with a CH...O distance of 2.173 Å [cc-pVTZ, 2.171 Å with the 6-311++G-(3df,3pd) basis]. Additional stabilization of the complex is due to the C–H... $\pi$  interaction between the two acetylene molecules (contribution iii), which corresponds to the T shape of the acetylene dimer.<sup>21</sup> In this case, the T is distorted by interactions

**TABLE 4: Comparison of Selected Intramolecular Distances of the Formic Acid and Acetylene Monomers (M) and 1:2 Formic Acid/Acetylene Complexes A–C<sup>a</sup>**

	expt	MP2/cc-pVTZ				MP2/6-311++G(3df,3pd)			
	M	M	A	B	C	M	A	B	C
HCOOH									
$r(\text{C}=\text{O})$	1.202(10) <sup>b</sup>	1.203	1.209	1.211	1.205	1.202	1.207	1.209	1.204
$r(\text{O}—\text{H})$	0.972(5) <sup>b</sup>	0.969	0.978	0.977	0.979	0.968	0.976	0.975	0.977
$r(\text{C}—\text{O})$	1.343(10) <sup>b</sup>	1.346	1.333	1.332	1.342	1.343	1.331	1.331	1.339
C <sub>2</sub> H <sub>2</sub> (acetylene 1)									
$r(\text{C1}\equiv\text{C2})$	1.203 <sup>c</sup>	1.211	1.214	1.213	1.214	1.211	1.213	1.213	1.213
$r(\text{C1}—\text{H})$	1.062 <sup>c</sup>	1.061	1.067	1.064	1.064	1.062	1.067	1.064	1.064
$r(\text{C2}—\text{H})$			1.063	1.063	1.064		1.063	1.063	1.064
C <sub>2</sub> H <sub>2</sub> (acetylene 2)									
$r(\text{C3}\equiv\text{C4})$			1.213	1.213	1.213		1.213	1.212	1.212
$r(\text{C3}—\text{H})$			1.066	1.067	1.064		1.067	1.067	1.065
$r(\text{C4}—\text{H})$			1.062	1.062	1.062		1.062	1.062	1.062

<sup>a</sup> Distances given in Å. <sup>b</sup> Reference 54. <sup>c</sup> Reference 55.**TABLE 5: Calculated Vibrational Frequencies (in cm<sup>−1</sup>) of Complex A and Frequency Shifts Relative to the Isolated Monomer M (in Parentheses)**

B3LYP/6-311++G(d,p)		MP2/6-311++G(d,p)		MP2/cc-pVTZ		assignment
M	A	M	A	M	A	
3738.0	3583.2 (−155)	3797.2	3672.7 (−125)	3763.4	3604.9 (−159)	O—H stretch <sup>a</sup>
1816.2	1794.0 (−22)	1807.5	1795.3 (−12)	1818.1	1800.1 (−18)	C=O stretch <sup>a</sup>
1125.3	1167.3 (+42)	1142.6	1184.0 (+41)	1136.7	1183.9 (+47)	C—O stretch <sup>a</sup>
3057.5	3054.3 (−3)	3132.3	3126.4 (−6)	3125.1	3119.2 (−6)	C—H stretch <sup>a</sup>
3419.8	3379.2 (−41)	3455.2	3420.4 (−35)	3446.1	3397.0 (−49)	C—H stretch <sup>b</sup>
	3375.2 (−45)		3429.8 (−25)		3409.3 (−37)	
772.7	801.3 (+29)	766.3	789.7 (+23)	753.0	786.9 (+34)	CCH bend <sup>b</sup>
	819.5 (+47)		795.2 (+29)		791.8 (+39)	
	832.1 (+59)		809.9 (+44)		802.0 (+49)	
	835.0 (+62)		828.8 (+63)		806.3 (+53)	

<sup>a</sup> Formic acid modes in the complex. <sup>b</sup> Acetylene modes in the complex.

of the two acetylene molecules with the formic acid molecule. The acetylene–acetylene interaction is characterized by a CH $\cdots$ C3 distance of 2.505 Å (2.496 Å) and a CH $\cdots$ C4 distance of 2.836 Å (2.815 Å) at the MP2/cc-pVTZ [MP2/6-311++G-(3df,3pd)] level of theory. These distances are in agreement with the expectations for weak to moderate hydrogen bonds<sup>2</sup> and compare well with that of the undisturbed T-shaped acetylene dimer.<sup>21,22</sup>

Complexes **B** and **C** provide further evidence for O–H $\cdots\pi$ , C–H $\cdots\pi$ , and CH $\cdots$ O interactions (Figure 1). In complex **B**, the two molecules of acetylene do not interact directly (thus, contribution iii is absent), but both interact with the formic acid molecule via contributions iv and i. A type iv interaction is found between the C1 H atom and the carbonyl oxygen atom. However, the long C1H $\cdots$ O distance of 2.635 Å indicates that this interaction is rather weak. Even weaker, with a distance of 3.418 Å, is the CH $\cdots\pi$  interaction of type ii between the formyl H atom of formic acid and the acetylene  $\pi$  system.

Complex **C** shows an additional weak CH $\cdots$ O interaction between the hydroxyl oxygen atom of the formic acid molecule and the hydrogen atom of one of the acetylene molecules (contribution v). The other complexes, **D–G**, show C–H $\cdots\pi$  and CH $\cdots$ O interactions; however, in this case, the acidic hydroxyl hydrogen atom of the formic acid molecule is not involved, resulting in low overall binding energies.

Structures **B1**, **E1**, **G1**, and **H1** are artifacts of the inability of the B3LYP functional to handle weak C–H $\cdots\pi$  dispersive interactions. Geometry optimization at the MP2/cc-pVTZ level of theory results in the transformation of **B1** to **B**, **E1** to **C**, **G1** to **G**, and **H1** to **D** (Table 3). Thus, by comparison of complex **B** with structure **B1**, it is evident that weak C–H $\cdots\pi$  interactions between the formyl H atom of formic acid and the  $\pi$  system of

acetylene are not reproduced by the B3LYP functional. This result was also noted in the study of 1:1 formic acid/acetylene complexes.<sup>34</sup>

**Intramolecular Distances and Vibrational Frequencies.** The intermolecular interactions in the complexes result in a distortion of the monomer intramolecular distances and vibrational frequencies. Table 4 lists some selected bond distances of the formic acid and acetylene monomers and the **A–C**, 1:2 formic acid/acetylene complexes. For the monomers, the experimental values<sup>54,55</sup> are well reproduced by calculations at the MP2/cc-pVTZ and MP2/6-311++G(3df,3pd) levels of theory. The vibrational frequencies of the complexes calculated at various levels of theory are listed in Tables 5–12. The Dunning basis sets are expected to be most reliable, given that excellent agreement between theory and experiment was found at this level for the 1:1 complexes.<sup>34</sup>

The most perturbed vibrational modes in complexes **A–C** are the O–H stretching vibrations of the formic acid molecules (Tables 5–8). At the MP2/cc-pVTZ level of theory, the frequency shifts in the complexes are −159, −145, and −183 cm<sup>−1</sup> for trimers **A–C**, respectively. This result reflects the structures of complexes **A–C** (Figure 1), which all exhibit strong interactions between the OH hydrogen atom and the  $\pi$  system of acetylene 1. In complex **C**, with the largest frequency shift (−183 cm<sup>−1</sup>), an additional interaction of the OH oxygen atom with one hydrogen atom of acetylene 2 is found. The formation of the complexes results in an elongation of the OH bonds of nearly 0.01 Å (MP2/cc-pVTZ, Table 4).

The carbonyl stretching frequencies of the formic acid molecules are predicted to be shifted by −18, −31, and −14 cm<sup>−1</sup> in complexes **A–C**, respectively. This again reflects the CO $\cdots$ H interaction between the carbonyl oxygen atom and the



**TABLE 6: Calculated Vibrational Frequencies (in cm<sup>-1</sup>) and Frequency Shifts Relative to the Isolated Monomer (in Parentheses) of Complexes B and B1**

B3LYP/6-311++G(d,p)		MP2/6-311++G(d,p)		MP2/cc-pVTZ		assignment
M	B1	M	B1	M	B1	
3738.0	3586.4 (−152)	3797.2	3681.6 (−116)	3763.4	3618.4 (−145)	O–H stretch <sup>a</sup>
1816.2	1786.1 (−30)	1807.5	1788.6 (−19)	1818.1	1787.3 (−31)	C=O stretch <sup>a</sup>
1125.3	1172.8 (+48)	1142.6	1187.6 (+45)	1136.7	1186.7 (+50)	C–O stretch <sup>a</sup>
3057.5	3057.7 (+0.2)	3132.3	3128.3 (−4)	3125.1	3121.4 (−4)	C–H stretch <sup>a</sup>
3419.8	3370.6 (−49)	3455.2	3417.9 (−37)	3446.1	3393.7 (−52)	C–H stretch <sup>b</sup>
	3404.1 (−16)		3442.0 (−13)		3429.4 (−17)	
772.7	791.7 (+19)	766.3	780.4 (+14)	753.0	767.6 (+15)	CCH bend <sup>b</sup>
	795.8 (+23)		782.6 (+16)		785.7 (+33)	
	838.5 (+66)		869.2 (+101)		796.2 (+43)	
	841.0 (+68)		872.6 (+106)		816.9 (+64)	

<sup>a</sup> Formic acid modes in the complex. <sup>b</sup> Acetylene modes in the complex.**TABLE 7: Calculated Vibrational Frequencies (in cm<sup>-1</sup>) of Complex C and Frequency Shifts Relative to the Isolated Monomer (in Parentheses)**

B3LYP/6-311++G(d,p)		MP2/6-311++G(d,p)		MP2/cc-pVTZ		assignment
M	C	M	C	M	C	
3738.0	3562.6 (−175)	3797.2	3650.7 (−147)	3763.4	3580.4 (−183)	O–H stretch <sup>a</sup>
1816.2	1806.2 (−10)	1807.5	1798.8 (−9)	1818.1	1804.2 (−14)	C=O stretch <sup>a</sup>
1125.3	1153.0 (+28)	1142.6	1168.9 (+26)	1136.7	1171.5 (+35)	C–O stretch <sup>a</sup>
3057.5	3048.1 (−9)	3132.3	3121.2 (−11)	3125.1	3114.9 (−10)	C–H stretch <sup>a</sup>
3419.8	3396.0 (−24)	3455.2	3434.4 (−21)	3446.1	3422.6 (−24)	C–H stretch <sup>b</sup>
	3400.0 (−20)		3435.7 (−20)		3424.2 (−22)	
772.7	790.0 (+17)	766.3	779.9 (+14)	753.0	767.5 (+15)	CCH bend <sup>b</sup>
	797.4 (+25)		788.2 (+22)		771.2 (+18)	
	805.2 (+33)		800.9 (+35)		789.9 (+37)	
	813.4 (+41)		802.2 (+36)		794.3 (+41)	

<sup>a</sup> Formic acid modes in the complex. <sup>b</sup> Acetylene modes in the complex.**TABLE 8: Experimental (Ar Matrix at 30–10 K) and Calculated [MP2/cc-pVTZ and B3LYP/6-311++G(d,p)] Vibrational Frequencies (in cm<sup>-1</sup>) of Formic Acid/Acetylene 1:2 Complex A and Frequency Shifts Δν in the Complex Relative to the Isolated Monomers (in Parentheses)**

experimental		calculated				assignment
		MP2/ cc-pVTZ		B3LYP/6-311++G(d,p)		
monomer	complex <b>A</b>	monomer	complex <b>A</b>	monomer	complex <b>A</b>	
3550.4	3395.0 (−155)	3763.4	3604.9 (−159)	3738.0	3583.2 (−155)	O–H stretch <sup>a</sup>
1767.1	1747.1 (−20)	1818.1	1800.1 (−18)	1816.2	1794.0 (−22)	C=O stretch <sup>a</sup>
1103.5	1145.4 (+42)	1136.7	1183.9 (+47)	1125.5	1167.3(+42)	C–O stretch <sup>a</sup>
3288.8	3244.5 (−44)	3446.1	3409.3 (−37)	3419.8	3379.2 (−41)	C–H stretch <sup>b</sup>
	3236.9 (−52)		3397.0 (−49)		3375.2 (−45)	

<sup>a</sup> Formic acid modes in the complex. <sup>b</sup> Acetylene modes in the complex.**TABLE 9: Calculated Vibrational Frequencies (in cm<sup>-1</sup>) of Complex D and Frequency Shift in the Complex Relative to the Isolated Monomer (in Parentheses)**

B3LYP/6-311++G(d,p)		MP2/6-311++G(d,p)		MP2/cc-pVTZ		assignment
M	D	M	D	M	D	
3738.0	3734.3 (−4)	3797.2	3792.5 (−5)	3763.4	3757.9 (−6)	O–H stretch <sup>a</sup>
1816.2	1794.4 (−22)	1807.5	1791.5 (−16)	1818.1	1797.5 (−21)	C=O stretch <sup>a</sup>
1125.3	1137.8 (+13)	1142.6	1153.3 (+11)	1136.7	1147.7 (+11)	C–O stretch <sup>a</sup>
3057.5	3076.2 (+19)	3132.3	3156.7 (+24)	3125.1		C–H stretch <sup>a</sup>
3419.8	3364.5 (−55)	3455.2	3408.6 (−47)	3446.1	3385.3 (−61)	C–H stretch <sup>b</sup>
	3389.7 (−30)		3431.4 (−24)		3409.4 (−37)	
772.7	792.8 (+20)	766.3	794.4 (+28)	753.0	770.8 (+18)	CCH bend <sup>b</sup>
	806.9 (+34)		810.5 (+44)		791.7 (+39)	
	842.3 (+70)		834.7 (+68)		802.6 (+50)	
	846.8 (+74)		843.3 (+77)		819.3 (+66)	

<sup>a</sup> Formic acid modes in the complex. <sup>b</sup> Acetylene modes in the complex.

acetylene H atom (contribution iv). In complex **B**, with a red shift (−31 cm<sup>-1</sup>) almost twice as large as those in complexes **A** and **C**, there is an additional CO⋯H interaction of the carbonyl group with the H atom of acetylene 2. This interaction results in a larger increase of the C=O bond length in **B** than in **A** and **C**.

The C–OH stretching modes of formic acid are blue-shifted in the complexes, and the C–OH formic acid bond lengths are consequently shorter than those in the monomer. Again, trimer **B** shows a larger blue shift (+50 cm<sup>-1</sup>) than complexes **A** and **C** (+47 cm<sup>-1</sup> and +35 cm<sup>-1</sup>, respectively), which can be associated with the very weak CH⋯π interaction between the

**TABLE 10: Calculated Vibrational Frequencies (in  $\text{cm}^{-1}$ ) of Complex E1 and Frequency Shifts Relative to the Isolated Monomer (in Parentheses)**

B3LYP/6-311++G(d,p)		MP2/6-311++G(d,p)		assignment
M	E1	M	E1	
3738.0	3626.2 (−112)	3797.2	3713.6 (−84)	O–H stretch <sup>a</sup>
1816.2	1798.0 (−18)	1807.5	1796.4 (−11)	C=O stretch <sup>a</sup>
1125.3	1155.2 (+30)	1142.6	1170.3 (+28)	C–O stretch <sup>a</sup>
3057.5	3052.9 (−5)	3132.3	3125.2 (−7)	C–H stretch <sup>a</sup>
3419.8	3397.5 (−22)	3455.2	3436.0 (−19)	C–H stretch <sup>b</sup>
	3408.4 (−11)		3448.5 (−7)	
772.7	783.0 (+10)	766.3	777.6 (+11)	CCH bend <sup>b</sup>
	790.9 (+18)		788.6 (+22)	
	793.8 (+21)		810.2 (+44)	
	807.8 (+35)		816.7 (+50)	

<sup>a</sup> Formic acid modes in the complex. <sup>b</sup> Acetylene modes in the complex

**TABLE 11: Calculated MP2 Vibrational Frequencies (in  $\text{cm}^{-1}$ ) of Complex F and Frequency Shifts Relative to the Isolated Monomer (in Parentheses)**

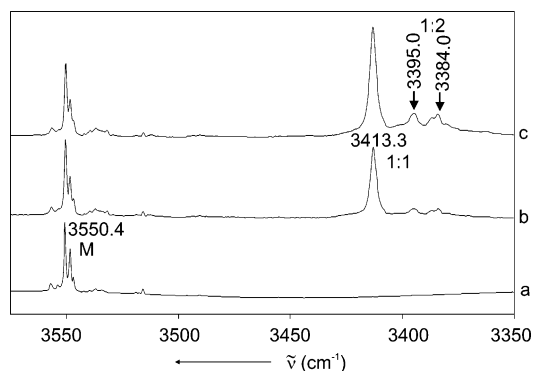
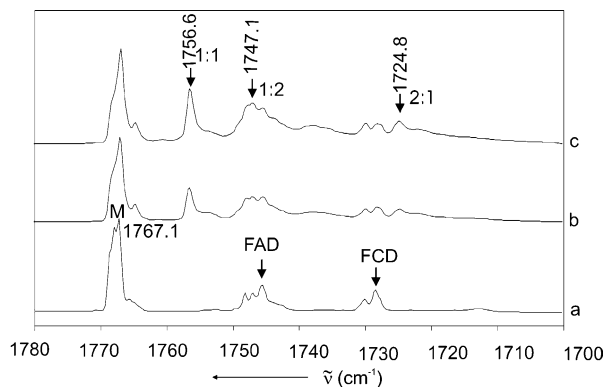
B3LYP/6-311++G(d,p)		MP2/6-311++G(d,p)		assignment
M	F	M	F	
3738.0	3734.9 (−3)	3797.2	3788.9 (−8)	O–H stretch <sup>a</sup>
1816.2	1817.0 (+1)	1807.5	1805.8 (−2)	C=O stretch <sup>a</sup>
1125.3	1108.9 (−16)	1142.6	1122.4 (−20)	C–O stretch <sup>a</sup>
3057.5		3132.3		C–H stretch <sup>a</sup>
3419.8	3388.8 (−31)	3455.2	3435.8 (−19)	C–H stretch <sup>b</sup>
	3397.5 (−22)		3429.6 (−25)	
772.7	788.6 (+16)	766.3	788.7 (+22)	CCH bend <sup>b</sup>
	801.3 (+29)		803.5 (+37)	
	813.6 (+41)		828.9 (+63)	
	829.2 (+57)		841.0 (+75)	

<sup>a</sup> Formic acid modes in the complex. <sup>b</sup> Acetylene modes in the complex.

CH group of the formic acid and the  $\pi$  system of acetylene 2 (contribution ii).

The C–H stretching modes of the acetylene moieties are also perturbed in the complexes. At the MP2/cc-pVTZ level of theory, these bands are red-shifted by  $-49$  and  $-37$   $\text{cm}^{-1}$  in trimer A, by  $-52$  and  $-17$   $\text{cm}^{-1}$  in complex B, and by  $-24$  and  $-22$   $\text{cm}^{-1}$  in complex C.

**Matrix Isolation Studies.** Matrix isolation experiments were performed to identify the trimers between one molecule of formic acid and two molecules of acetylene. The experiments were performed by matrix isolation of mixtures of formic acid and acetylene at various ratios in a large excess of argon at 10 K. Typical argon-to-sample ratios ranged from 600:1 to 600:1.5 for formic acid and from 600:1 to 600:2 for acetylene. Under these conditions (high dilution in argon and slow deposition),

**Figure 3.** Matrix isolation IR spectra in the O–H stretching region of formic acid. (a) HCOOH/Ar = 1:600. (b) HCOOH/C<sub>2</sub>H<sub>2</sub>/Ar = 1:1:600. (c) HCOOH/C<sub>2</sub>H<sub>2</sub>/Ar = 1:2:600.**Figure 4.** Matrix isolation IR spectra in the C=O stretching region of formic acid. (a) HCOOH/Ar = 1:400. (b) HCOOH/C<sub>2</sub>H<sub>2</sub>/Ar = 1:1:600. (c) HCOOH/C<sub>2</sub>H<sub>2</sub>/Ar = 1:2:600. FAD, nonsymmetrical (acyclic) formic acid dimer; FCD, cyclic formic acid dimer.

mainly monomers of formic acid and acetylene were formed. Subsequent annealing of the matrix at temperatures up to 30 K resulted in the formation of complex mixtures of aggregates. The main constituents of these mixtures had been identified previously: the acetylene dimer,<sup>56–58</sup> the formic acid dimer,<sup>28,29,32</sup> and the 1:1 complex between acetylene and formic acid.<sup>34</sup> Careful analysis of the IR absorptions revealed the formation of several new bands that could not be assigned to any of the previously known species (Table 8).

Figures 3–5 show the vibrational modes corresponding to O–H, C=O, and C–O, respectively, stretching regions of formic acid upon co-deposition of formic acid, acetylene, and argon in 1:1:600 and 1:2:600 molar ratios. The blank spectrum of formic acid is also included for comparison. All spectra displayed in this paper were obtained after the matrix had been

**TABLE 12: Calculated Vibrational Frequencies (in  $\text{cm}^{-1}$ ) of Complex G (or G1) and Frequency Shifts Relative to the Isolated Monomer (in Parentheses)**

B3LYP/6-311++G(d,p)		MP2/6-311++G(d,p)		MP2/cc-pVTZ		assignment
M	G1	M	G	M	G	
3738.0	3735.0 (−3)	3797.2	3795.8 (−1)	3763.4	3760.5 (−3)	O–H stretch <sup>a</sup>
1816.2	1805.7 (−11)	1807.5	1798.2 (−9)	1818.1	1803.4 (−15)	C=O stretch <sup>a</sup>
1125.3	1138.3 (+13)	1142.6	1150.5 (+8)	1136.7	1147.4 (+11)	C–O stretch <sup>a</sup>
3057.5	3066.5 (+9)	3132.3	3141.0 (+9)	3125.1	3133.9 (+9)	C–H stretch <sup>a</sup>
3419.8	3371.8 (−48)	3455.2	3452.2 (−3)	3446.1	3395.6 (−51)	C–H stretch <sup>b</sup>
	3416.8 (−3)		3424.4 (−31)		3440.5 (−6)	
772.7	774.0 (+1)	766.3	764.8 (−2)	753.0	753.5 (+1)	CCH bend <sup>b</sup>
	779.4 (+7)		769.3 (+3)		759.0 (+6)	
	837.4 (+65)		814.1 (+48)		806.9 (+54)	
	842.6 (+70)		831.3 (+65)		807.9 (+55)	

<sup>a</sup> Formic acid modes in the complex. <sup>b</sup> Acetylene modes in the complex.

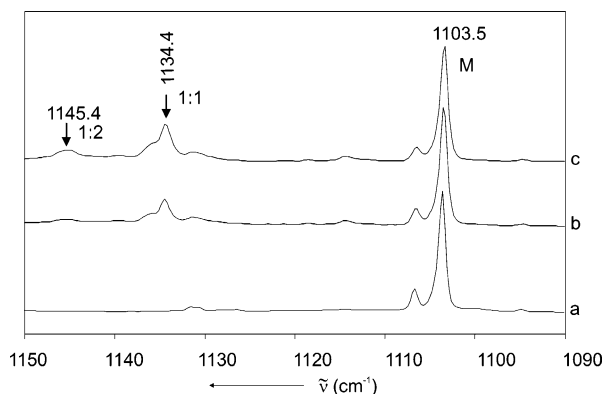


**Figure 5.** Matrix isolation IR spectra in the C–O stretching region of formic acid. (a) HCOOH/Ar = 1:600. (b) HCOOH/C<sub>2</sub>H<sub>2</sub>/Ar = 1:1:600. (c) HCOOH/C<sub>2</sub>H<sub>2</sub>/Ar = 1:2:600.

annealed at 30 K. At higher acetylene concentrations, two new peaks were observed in the O–H stretching region at 3395.0 and 3384.0 cm<sup>−1</sup>. Because the intensity of these bands increased with increasing acetylene concentration more than that of the 1:1 complexes, they were tentatively assigned to the O–H stretching vibration of formic acid in a 1:2 complex of formic acid and acetylene. The doublet structure could be caused by matrix site effects, similarly to the triplet structure observed for the O–H stretching vibration of formic acid in an argon matrix.<sup>59</sup> The experimental frequency shift (−155 cm<sup>−1</sup>) is in excellent agreement with the calculated frequency shifts [−159 cm<sup>−1</sup> with MP2/cc-pVTZ and −155 with B3LYP/6-311++G(d,p)] for complex **A** (Table 8).

In the C=O stretching region, increasing acetylene concentration results in an increase of the intensity of the band at 1747 cm<sup>−1</sup> assigned to the less stable, unsymmetrical formic acid dimer. In addition, this absorption broadens significantly. This indicates that, in addition to the formic acid dimer, a new species assigned to the 1:2 complex of formic acid and acetylene is formed under these conditions. The intensity of this band depends on the acetylene concentration, in agreement with the assignment to the C=O stretching vibration of the 1:2 complex **A**. The good agreement between the experimental frequency shift (−20 cm<sup>−1</sup>) and the calculated values [−18 cm<sup>−1</sup> with MP2/cc-pVTZ and −22 with B3LYP/6-311++G(d,p)] further confirms the formation of complex **A**.

In the C–O stretching region, a new band appears at 1145.4 cm<sup>−1</sup> at higher acetylene concentration. By comparison with the calculated frequencies, this band is also assigned to the 1:2 complex **A**. The experimental frequency shift (+42 cm<sup>−1</sup>) is in excellent agreement with the B3LYP/6-311++G(d,p) (+42) and MP2/cc-pVTZ (+47) values.

When acetylene and formic acid are co-deposited, two new bands in the acetylene C–H stretching region at 3244.5 and 3236.9 cm<sup>−1</sup> are observed in addition to the previously assigned absorptions<sup>56–58</sup> (Figure 6). The intensity of these new absorptions increases as the acetylene concentration increases, in agreement with the expectation for a formic acid/acetylene 1:2 complex. The experimental frequency shifts (−44 and −52 cm<sup>−1</sup>) are in reasonable agreement with the calculated shifts for complex **A** [−37, −49 cm<sup>−1</sup> with MP2/cc-pVTZ and −41, −45 cm<sup>−1</sup> with B3LYP/6-311++G(d,p), Table 8]. In the CCH bending region of acetylene, the 1:2 complex absorptions are too weak to be observed.

#### Analysis of the Intermolecular Interactions in the Trimers.

To quantify the contributions of intermolecular interactions in trimers **A–C**, we sequentially removed one of the three

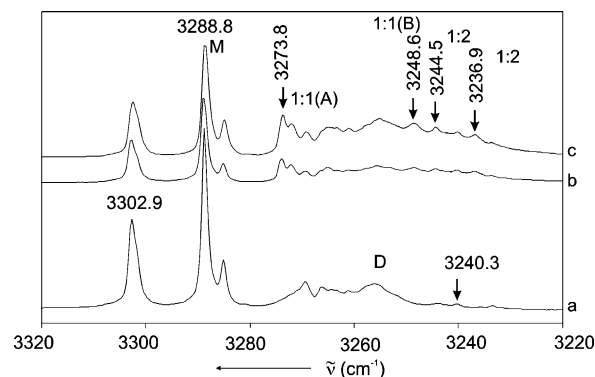


**Figure 6.** Matrix isolation IR spectra in the C–H stretching region of acetylene. (a) C<sub>2</sub>H<sub>2</sub>/Ar = 1:300. (b) HCOOH/C<sub>2</sub>H<sub>2</sub>/Ar = 1:1:600. (c) HCOOH/C<sub>2</sub>H<sub>2</sub>/Ar = 1:2:600.

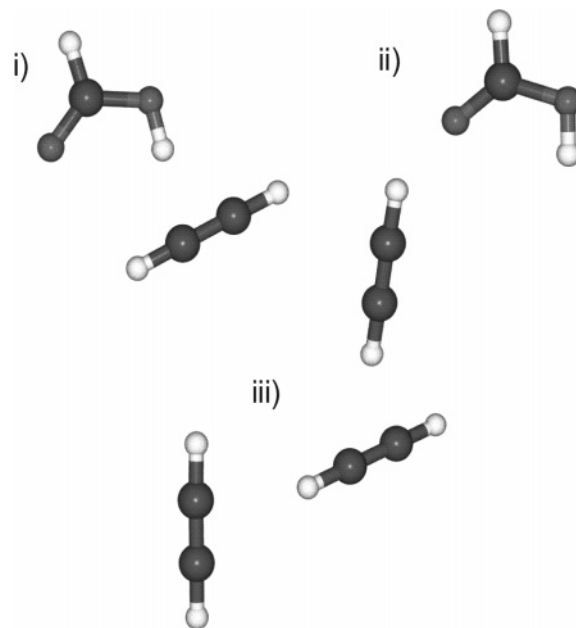


**Figure 7.** Dimers of complex **A**. Partial structure i: Formic acid and acetylene 1. Partial structure ii: Formic acid and acetylene 2. Partial structure iii: acetylene 1 and acetylene 2.

monomers (formic acid or one of the two acetylene molecules) from each of the trimers. The energies of the remaining partial structures (remaining dimers) were calculated (MP2/cc-pVTZ) in the geometries of the parent trimers (Figure 7). These partial structures were then compared with the optimized dimers to analyze the influence of the third molecule in the trimer on the dimer structures. From that analysis, we obtained a detailed picture of the noncovalent interactions in an aggregate consisting of three components.

In trimer **A**, the first partial structure is formed by removing acetylene 2 and thus consists of formic acid and the remaining acetylene 1 (partial structure i) interacting via noncovalent bond contribution i. Analogously, partial structure ii is formed by removing acetylene 1 and consists of formic acid and acetylene 2 interacting via contribution iv. Finally, partial structure iii results from removing the formic acid molecule and represents the (more or less distorted) T-shaped acetylene dimer interacting via contribution iii. Partial structures i–iii in trimers **B** and **C** are formed analogously by sequentially removing acetylene 2, acetylene 1, and the formic acid molecule.

Several nonadditive contributions have to be taken into account that might contribute to the stabilization of the trimers (Table 13). These nonadditive contributions are obtained by

**TABLE 13: MP2/cc-pVTZ Energies of Trimers A–C and Their Partial Structures i, ii, and iii (in kcal/mol)**

acetylene/formic acid 2:1 complex $E(t)$	A	B	C
partial structure i, $E(i)$	−4.62 (48.5%)	−5.18 (59.1%)	−4.97 (59.0%)
partial structure ii, $E(ii)$	−2.67 (28.1%)	−3.33 (38.0%)	−1.73 (20.5%)
partial structure iii, $E(iii)$	−1.39 (14.6%)	+0.11 (1.2%)	−1.35 (16.0%)
$E(t) - [E(i) + E(ii) + E(iii)]$	−0.84 (8.8%)	−0.37 (4.2%)	−0.37 (4.4%)

**TABLE 14: Calculated Binding Energies (in kcal/mol) of the Acetylene Dimer<sup>a</sup> and the  $C_{2v}$  Acetylene Dimer**

	MP2/6-311++G(3df,3pd)	MP2/cc-pVTZ
acetylene dimer <sup>a</sup>	−1.61	−1.39
$C_{2v}$ acetylene dimer <sup>b</sup>	−1.86	−1.63

<sup>a</sup> Complex A, partial structure iii. <sup>b</sup> Reference 21.

subtracting all dimer binding energies from the trimer binding energy. As can be seen from Table 13, the nonadditive contributions are small.

In all complexes, partial structure i contributes most to the trimer energies. The “strongest” O–H $\cdots\pi$  interaction between formic acid and acetylene (contribution i) dominates the interaction in the trimer. In trimers B and C, where partial structure i contributes 59% to the total binding energy, an additional CH $\cdots$ O interaction between the carbonyl oxygen atom and one of the H atoms of acetylene 1 can be found (contribution iv). This increases the binding energy of this partial structure in trimers B and C compared to that in A (48.5%).

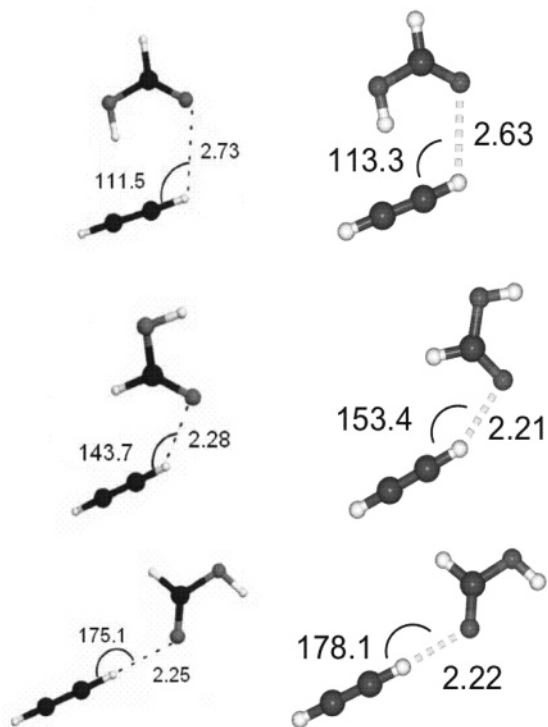


**Figure 8.** Comparison of 1:1 complexes of formic acid and acetylene with the partial structures of the 1:2 complexes. Left side: 1:1 complexes. Top, MP2/6-311++G(d,p); center, MP2/cc-pVTZ; bottom, MP2/6-311++G(d,p). Right side: Partial structures i and ii from 1:2 complexes B and B1, respectively. Top, partial structure i of complex B, MP2/cc-pVTZ; center, partial structure ii of complex B, MP2/cc-pVTZ; bottom, partial structure ii of complex B1, MP2/6-311++G(d,p).

Partial structure ii contributes differently to the three trimers: 28.1% in complex A (only contribution iv), 38.0% in complex B, and 20.5% in complex C. In B, the interaction of type iv is most important, but in this case, it is accompanied by a very weak interaction of type ii.

In complex B, a type iii interaction between the acetylene molecules is not possible, and only a very small repulsive interaction (1.2%) is observed. This is a consequence of repulsions between the closest hydrogen atoms in the two acetylene molecules.

For complex A, it is interesting to compare the calculated binding energies and geometries of the acetylene dimer from partial structure iii with those of the well-known  $C_{2v}$  acetylene dimer (Table 14).<sup>21</sup> The presence of formic acid results in a small destabilization of partial structure iii compared to the undistorted acetylene dimer by around 0.25 kcal/mol. For the  $C_{2v}$  acetylene dimer, the CH $\cdots$ C3 (and CH $\cdots$ C4) distance is 2.727 Å at the MP2/cc-pVTZ level of theory, whereas for partial structure iii, the CH $\cdots$ C3 distance is 2.505 Å, and the CH $\cdots$ C4 distance 2.836 Å.

Figure 8 shows the formic acid/acetylene dimers (left-hand side) compared to several partial structures i and ii (right-hand side). A comparison between these structures reveals interesting similarities between the partial structures and the dimers. Thus, the O–H $\cdots\pi$  bidentate 1:1 complex is very similar to partial structure i, and the structures of the CH $\cdots$ O=C bidentate and monodentate 1:1 complexes agree well with partial structures ii of the B and B1 trimers, respectively.

## Conclusion

Formic acid/acetylene is an interesting system to study noncovalent interactions, because a variety of “nonclassical” hydrogen bonds can be formed where four acidic hydrogen atoms (OH and CH at formic acid, two CH at acetylene) compete for the two oxygen atoms in formic acid and the acetylene  $\pi$  system as hydrogen-bond acceptors. The introduction of an additional acetylene molecule into the trimer complexes results in a number of energetically close-lying complexes that were analyzed at the B3LYP and MP2 levels of theory with large basis sets. The deficit of the B3LYP method and MP2 calculations with smaller basis sets to account for intermediate-range dispersive interactions results in the production of four artificial minima, B1, E1, G1, and H1, that disappear at the higher level of theory.

The interaction between the acidic H atom of formic acid and the acetylene  $\pi$  system (contribution i) provides 50–60% of the binding energies of the most stable complexes, A–C, and thus dominates the noncovalent interactions in these systems (Table 13). Contributions ii and iii add between 15 and 29%. Only in complex B, where no “T-acetylene” interaction is present, is contribution iii slightly repulsive. Other interactions are less important for the stabilization of the complexes, but might influence the structure. Thus, complex B is only slightly stabilized by an additional very weak CH $\cdots\pi$  interaction compared to B1. This interaction results in a considerable structural change (Figure 1). The most stable 1:2 complex, A, could also be characterized in argon matrix, as evidenced by the shifts in the vibrational frequencies of the formic acid and the acetylene fundamental modes. The experimental frequency shifts are in good agreement with the calculated shifts, supporting the appearance of the global minimum complex in the matrix.



**Acknowledgment.** This work was financially supported by the Deutsche Forschungsgemeinschaft (Sonderforschungsbereich 452) and the Fonds der Chemischen Industrie. We thank Dr. Holger Bettinger for helpful discussions.

## References and Notes

- (1) Jeffrey, G. A. *J. Molecular Structure* **1994**, 322, 21.
- (2) Jeffrey, G. A., Ed. *An Introduction to Hydrogen Bonding*; Oxford University Press: Oxford, U.K., 1997.
- (3) Nishio, M.; Hirota, M.; Umezawa, Y. *CH/ $\pi$  Interaction: Evidence, Nature, and Consequences*; Wiley: New York, 1998.
- (4) Zheng, Y. J.; Merz, K. M., Jr. *J. Comput. Chem.* **1992**, 13, 1151.
- (5) Spomer, J.; Hobza, P.; Leszczynski, J. *Comput. Chem. (Singapore)* **2000**, 5, 171.
- (6) Hartmann, M.; Wetmore, S. D.; Radom, L. *J. Phys. Chem. A* **2001**, 105, 4470.
- (7) Hobza, P.; Riehn, C.; Weichert, A.; Brutschy, B. *Chem. Phys.* **2002**, 283, 331.
- (8) Jeng, M. L. H.; Ault, B. S. *J. Phys. Chem.* **1990**, 94, 4851.
- (9) Jeng, M. L. H.; Ault, B. S. *J. Phys. Chem.* **1990**, 94, 1323.
- (10) Tsuzuki, S.; Honda, K.; Uchimaru, T.; Mikami, M.; Tanabe, K. *J. Phys. Chem. A* **1999**, 103, 8265.
- (11) Hobza, P.; Selzle, H. L.; Schlag, E. W. *Collect. Czech. Chem. Commun.* **1992**, 57, 1186.
- (12) Petrusova, H.; Havlas, Z.; Hobza, P.; Zahradnik, R. *Collect. Czech. Chem. Commun.* **1988**, 53, 2495.
- (13) Maier, G.; Lautz, C. *European J. Org. Chem.* **1998**, 769.
- (14) Lukes, V.; Breza, M. *Pet. Coal* **2002**, 44, 51.
- (15) Muentner, J. S. *J. Chem. Phys.* **1991**, 94, 2781.
- (16) Craw, J. S.; Nascimento, M. A. C.; Ramos, M. N. *Spectrochim. Acta A: Mol. Biomol. Spectrosc.* **1991**, 47, 69.
- (17) Scheiner, S.; Grabowski, S. J. *J. Mol. Struct.* **2002**, 615, 209.
- (18) Resende, S. M.; De Almeida, W. B. *Chem. Phys.* **1996**, 206, 1.
- (19) Dykstra, C. E. *J. Am. Chem. Soc.* **1990**, 112, 7540.
- (20) Shuler, K.; Dykstra, C. E. *J. Phys. Chem. A* **2000**, 104, 11522.
- (21) Karpfen, A. *J. Phys. Chem. A* **1999**, 103, 11431.
- (22) Prichard, D. G.; Nandi, R. N.; Muentner, J. S. *J. Chem. Phys.* **1988**, 89, 115.
- (23) Craw, J. S.; De Almeida, W. B.; Hinchliffe, A. *THEOCHEM* **1989**, 60, 69.
- (24) Aoyama, T.; Matsuoka, O.; Nakagawa, N. *Chem. Phys. Lett.* **1979**, 67, 508.
- (25) Alberts, I. L.; Rowlands, T. W.; Handy, N. C. *J. Chem. Phys.* **1988**, 88, 3811.
- (26) Borisenko, K. B.; Bock, C. W.; Hargittai, I. *THEOCHEM* **1995**, 332, 161.
- (27) Brinkmann, N. R.; Tschumper, G. S.; Yan, G.; Schaefer, H. F. *J. Phys. Chem. A* **2003**, 107, 10208.
- (28) Halupka, M.; Sander, W. *Spectrochim. Acta A: Mol. Biomol. Spectrosc.* **1998**, 54, 495.
- (29) Gantenberg, M.; Halupka, M.; Sander, W. *Chem.—Eur. J.* **2000**, 6, 1865.
- (30) Hayashi, S.; Umemura, J.; Kato, S.; Morokuma, K. *J. Phys. Chem.* **1984**, 88, 1330.
- (31) Flood, E. J. *J. Mol. Struct.* **1974**, 21, 221.
- (32) Reva, I. D.; Plokhotnichenko, A. M.; Radchenko, E. D.; Sheina, G. G.; Blagoi, Y. P. *Spectrochim. Acta A: Mol. Biomol. Spectrosc.* **1994**, 50, 1107.
- (33) Ushiyama, H.; Takatsuka, K. *J. Chem. Phys.* **2001**, 115, 5903.
- (34) George, L.; Sanchez-Garcia, E.; Sander, W. *J. Phys. Chem. A* **2003**, 107, 6850.
- (35) Montero, L. A.; Esteva, A. M.; Molina, J.; Zapardiel, A.; Hernandez, L.; Marquez, H.; Acosta, A. *J. Am. Chem. Soc.* **1998**, 120, 12023.
- (36) Montero, L. A.; Molina, J.; Fabian, J. *Int. J. Quantum Chem.* **2000**, 79, 8.
- (37) Stewart, J. J. P. *J. Comput. Chem* **1989**, 10, 210.
- (38) Dewar, M. J. S.; E. G. Z.; Healy, E. F.; Stewart, J. J. P. *J. Am. Chem. Soc.* **1985**, 107, 3902.
- (39) Stewart, J. J. P. MOPAC Versions 6 and 7.
- (40) Csonka, G. I. *J. Comput. Chem.* **1993**, 14, 895.
- (41) Csonka, G. I.; Angyan, J. G. *Theochem* **1997**, 393, 31.
- (42) Turi, L.; Dannenberg, J. J. *J. Phys. Chem.* **1993**, 97, 7899.
- (43) Frisch, M. J.; Trucks, G. W.; Schlegel, H. B.; Scuseria, G. E.; Robb, M. A.; Cheeseman, J. R.; Zakrzewski, V. G.; Montgomery, J. A., Jr.; Stratmann, R. E.; Burant, J. C.; Dapprich, S.; Millam, J. M.; Daniels, A. D.; Kudin, K. N.; Strain, M. C.; Farkas, O.; Tomasi, J.; Barone, V.; Cossi, M.; Cammi, R.; Mennucci, B.; Pomelli, C.; Adamo, C.; Clifford, S.; Ochterski, J.; Petersson, G. A.; Ayala, P. Y.; Cui, Q.; Morokuma, K.; Malick, D. K.; Rabuck, A. D.; Raghavachari, K.; Foresman, J. B.; Cioslowski, J.; Ortiz, J. V.; Stefanov, B. B.; Liu, G.; Liashenko, A.; Piskorz, P.; Komaromi, I.; Gomperts, R.; Martin, R. L.; Fox, D. J.; Keith, T.; Al-Laham, M. A.; Peng, C. Y.; Nanayakkara, A.; Gonzalez, C.; Challacombe, M.; Gill, P. M. W.; Johnson, B.; Chen, W.; Wong, M. W.; Andres, J. L.; Head-Gordon, M.; Replogle, E. S.; Pople, J. A. *Gaussian 98*, revision A.3; Gaussian, Inc.: Pittsburgh, PA, 1998.
- (44) Frisch, M. J.; Trucks, G. W.; Schlegel, H. B.; Scuseria, G. E.; Robb, M. A.; Cheeseman, J. R.; Montgomery, J. A., Jr.; Vreven, T.; Kudin, K. N.; Burant, J. C.; Millam, J. M.; Iyengar, S. S.; Tomasi, J.; Barone, V.; Mennucci, B.; Cossi, M.; Scalmani, G.; Rega, N.; Petersson, G. A.; Nakatsuji, H.; Hada, M.; Ehara, M.; Toyota, K.; Fukuda, R.; Hasegawa, J.; Ishida, M.; Nakajima, T.; Honda, Y.; Kitao, O.; Nakai, H.; Klene, M.; Li, X.; Knox, J. E.; Hratchian, H. P.; Cross, J. B.; Adamo, C.; Jaramillo, J.; Gomperts, R.; Stratmann, R. E.; Yazyev, O.; Austin, A. J.; Cammi, R.; Pomelli, C.; Ochterski, J. W.; Ayala, P. Y.; Morokuma, K.; Voth, G. A.; Salvador, P.; Dannenberg, J. J.; Zakrzewski, V. G.; Dapprich, S.; Daniels, A. D.; Strain, M. C.; Farkas, O.; Malick, D. K.; Rabuck, A. D.; Raghavachari, K.; Foresman, J. B.; Ortiz, J. V.; Cui, Q.; Baboul, A. G.; Clifford, S.; Cioslowski, J.; Stefanov, B. B.; Liu, G.; Liashenko, A.; Piskorz, P.; Komaromi, I.; Martin, R. L.; Fox, D. J.; Keith, T.; Al-Laham, M. A.; Peng, C. Y.; Nanayakkara, A.; Challacombe, M.; Gill, P. M. W.; Johnson, B.; Chen, W.; Wong, M. W.; Gonzalez, C.; Pople, J. A. *Gaussian 03*, revision B.03; Gaussian, Inc.: Pittsburgh, PA, 2003.
- (45) Werner, H.-J.; Knowles, P. J.; Schütz, M.; Lindh, R.; Celani, P.; Korona, T.; Rauhut, G.; Manby, F. R.; Amos, R. D.; Bernhardsson, A.; Berning, A.; Cooper, D. L.; Deegan, M. J. O.; Dobbyn, A. J.; Eckert, F.; Hampel, C.; Hetzer, G.; Lloyd, A. W.; McNicholas, S. J.; Meyer, W.; Mura, M. E.; Nicklass, A.; Palmieri, P.; Pitzer, R.; Schumann, U.; Stoll, H.; Stone, A. J.; Tarroni, R.; Thorsteinsson, T. *MOLPRO*; Universität Stuttgart: Stuttgart, Germany.
- (46) Moller, C.; Plesset, M. S. *Phys. Rev.* **1934**, 46, 618.
- (47) Becke, A. D. *J. Chem. Phys.* **1993**, 98, 5648.
- (48) Lee, C.; Yang, W.; Parr, R. G. *Phys. Rev. B: Condens. Matter Mater. Phys.* **1988**, 37, 785.
- (49) Raghavachari, K.; G. W. T.; Pople, J. A.; Head-Gordon, M. *Chem. Phys. Lett.* **1989**, 157, 479.
- (50) Frisch, M. J.; Pople, J. A.; Binkley, J. S. *J. Chem. Phys.* **1984**, 80, 3265.
- (51) Krishnan, R.; Binkley, J. S.; Seeger, R.; Pople, J. A. *J. Chem. Phys.* **1980**, 72, 650.
- (52) Dunning, T. H., Jr. *J. Chem. Phys.* **1989**, 90, 1007.
- (53) Boys, S. F.; Bernardi, F. *Mol. Phys.* **1970**, 19, 553.
- (54) Harmony, M. D.; Laurie, V. W.; Kuczkowski, R. L.; Schwendeman, R. H.; Ramsay, D. A.; Lovas, F. J.; Lafferty, W. J.; Maki, A. G. *J. Phys. Chem. Ref. Data* **1979**, 8, 619.
- (55) Baldacci, A.; Ghergetti, S.; Hurlock, S. C.; Rao, K. N. *J. Mol. Spectrosc.* **1976**, 59, 116.
- (56) Kline, E. S.; Kafafi, Z. H.; Hauge, R. H.; Margrave, J. L. *J. Am. Chem. Soc.* **1985**, 107, 7559.
- (57) McDonald, S. A.; Johnson, G. L.; Keelan, B. W.; Andrews, L. *J. Am. Chem. Soc.* **1980**, 102, 2892.
- (58) Jemmis, E. D.; Giju, K. T.; Sundararajan, K.; Sankaran, K.; Vidya, V.; Viswanathan, K. S.; Leszczynski, J. *J. Mol. Struct.* **1999**, 510, 59.
- (59) Lundell, J.; Raesaenen, M.; Latajka, Z. *Chem. Phys.* **1994**, 189, 245.